forum acusticum 2026
8-12 September · Graz, Austria

A STUDY OF THE RELATIONSHIP BETWEEN TRAIN SPEED AND ACCELERATION AMPLITUDE BASED ON ABA MEASUREMENTS

Helena Steine Tysland[1], Albert Lau[2], Torbjørn Ursin[3]
[1,2] *Department of Civil and Environmental Engineering, NTNU, Norway*
[3] *Bane NOR, Schweigaards gate 33, 0191 Oslo, Norway*

This contribution has been accepted based on the submitted abstract. The submitted manuscript was not reviewed and is reproduced here without edits or corrections by the conference board. Neither the EAA nor the AAA take responsibility for its contents.

Abstract

This paper investigates the relationship between train speed and acceleration amplitude measured through axle-box acceleration (ABA) at insulated rail joints (IRJs) on the Norwegian railway network, using the track-recording vehicle Roger 1000. A total of 56 passages (from two IRJs) recorded with a tri-axial piezoelectric accelerometer mounted near the axle box on the leading wheelset were analyzed. For each passage, a ± 2.5 s window around the IRJ was extracted to identify the exact peak where the train is assumed to have passed the IRJ, and a RMS-value of the absolute amplitudes was computed in a ± 1 ms gliding window to show the local vibration energy. Second-order regression models were fitted for both vertical and longitudinal directions that show a near-linear increase in amplitude with speed, with the vertical direction exhibiting the highest sensitivity. Further, normalized RMS values with speed based on the second order regressions help reveal outliers from a perfect amplitude-speed-relationship, indicating additional influences. The longitudinal (X) direction exhibits larger relative variability than the vertical response after speed normalization, and the changes following documented rail-grinding events were more pronounced in X-direction, suggesting that longitudinal accelerations are more sensitive to subtle changes in track condition.

Keywords: *railway monitoring, axle-box acceleration (ABA), insulated rail joints (IRJs), track condition*

1. Introduction

Track maintenance is essential for safe and reliable railway operations, as effective maintenance practices are crucial for improving passenger safety and comfort [1]. Traditional maintenance through manual inspections has made it difficult to detect early-stage defects before they affect train operations [2].
Real-time continuous railway monitoring with smart sensors represents a major improvement over traditional inspections, enabling earlier detection of track defects [3]. Train-mounted accelerometers are among the most promising tools for condition monitoring [4].

1.1. Literature review

Mounting sensors on regular trains has gained increasing attention, as this enables continuous measurements during normal operations and supports both vehicle and track monitoring [1]. Axle-box accelerations (ABA) are particularly useful for detecting track defects, as the sensors capture a broad frequency range [4]. Higher speeds and shorter wavelengths generate higher excitation frequencies, and different components of the vehicle-track system respond in distinct frequency ranges [5]. Low-frequency signals (> 2 m wavelength) indicate large-scale geometric deviations, while high-frequency content indicates local defects such as squats or irregularities at joints [4].
Several studies have applied advanced data analysis to ABA measurements. ABA has detected squats and switch defects using wavelet-based approaches and unsupervised learning by exploiting localized frequency responses [6, 7]. Yang et al. showed that joints and other defects can be detected from raw acceleration signals using deep learning [8]. A study analyzing ABA on high-speed trains (∼300 km/h) found that longitudinal ABA produced stronger responses (∼1.4 times higher) than vertical ABA for the same rail defect and was more effective for detecting local squats. Longitudinal ABA does not include vibrations from fasteners and sleepers, in contrast to vertical ABA, and therefore captures the vibration response from the rail impact more effectively [6].
IRJs are critical components due to their electrical and structural functions. Molodova et al. demonstrated

Corresponding author: *helena.tysland@gmail.com.*

that ABA measurements at wheelsets can detect IRJ defects, achieving 84% detection rate [9].
Optimal sensor placement and proper signal processing remain essential. Sensors mounted near the leading bogie or first wheelset provide the strongest responses [1]. At the same time, ABA amplitudes are strongly affected by train speed, complicating direct interpretation of raw measurements [10]. Filtering, time-frequency transforms and wavelet analysis are therefore necessary to extract reliable indicators of defect presence [11]. Overall, the literature highlights the potential of ABA measurements for condition-based maintenance, while highlighting several challenges.

1.2. Scope and contribution of this work

This paper investigates the speed-response relationship at two IRJs on the Norwegian network where Roger 1000 has passed at different times at different speeds. The objective is to quantify the relationship between speed and ABA amplitude and evaluate the variability across multiple passages. IRJs represent a clear vertical discontinuity, and require proper maintenance to withstand operational loads. Because this discontinuity produces a distinct impulsive response in ABA measurements [12], they were selected as suitable features for this study.
This paper addresses three research questions:

1. How sensitive is the vibration response at different speeds?
2. How does speed affect the amplitude when passing isolated rail joints?
3. How do variations in the condition of the track affect the relationship between speed and acceleration amplitude?

This paper contributes by presenting a structured methodology for ABA processing centered on IRJ passages, analyzing amplitude vs speed, quantifying variability and identifying outlier behavior to this relation, and discussing implications for ABA-based monitoring and recommendations for further research.

2. Methodology

2.1. Data description

ABA data were obtained from the Norwegian track recording vehicle Roger 1000, equipped with four piezoelectric tri-axial accelerometers Model 138.02 with dynamic range of 200g mounted on the axle-boxes of the bogies. Data were sampled at 20 kHz and extracted from the accelerometer installed near the axle-box of the leading wheelset on the left side, as sensors near leading wheelsets typically provide the strongest signals[1]. Data were collected from two positions with IRJs on a single-track section between Lillestrøm and Eidsvoll, eliminating inconsistencies that can occur on double-track lines. Both IRJs are located in an area with straight horizontal alignment. Position 1 has a vertical gradient of +3.5‰, and position 2 has a gradient of -10‰.

A total of 56 passages over two different IRJs (29 and 27 per IRJ), recorded between 2023 and 2025 (largely collected on the same days for both positions) at varying operating speeds were extracted and analyzed in vertical (Z) and longitudinal (X) direction. GNSS-based NMEA files provided speed, positional information and local time, which were synchronized with raw acceleration data containing amplitude signals. Figure 1 shows the configuration of the ABA measurement system used on Roger 1000, including sensor placement near the axle-box, GNSS on the roof, and signal transmission to the onboard data acquisition unit.

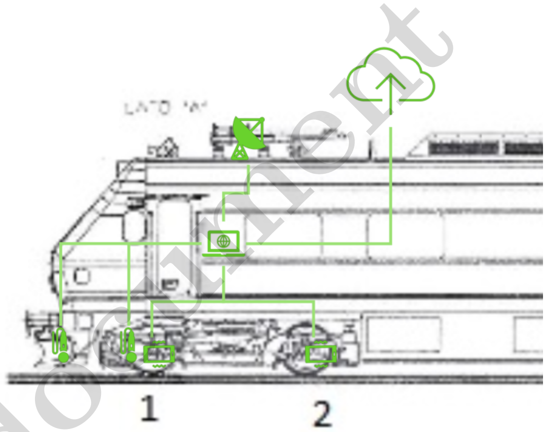

Figure 1: Illustration of the ABA measurement system. (T. Ursin, personal communication, May 7, 2025).

2.2. Data analysis

The analysis aimed to quantify the relationship between train speed and ABA response at IRJs and address the research questions on sensitivity, speed effect, and track variability.
IRJ positions were identified using GNSS coordinates with an accepted tolerance of approximately ±0.00004°latitude and ±0.00002°longitude, which corresponds to approximately 4.45 meters and 1.11 meters, respectively, to compensate for GNSS measurement deviations and ensure correct passage selection. For each passage, a ±2.5 s gliding window around the IRJ was extracted to capture the impact transient, as the distance between the GNSS antenna and the accelerometer introduces a positional offset of several meters along the track that needs to be accounted for. Within each window, the absolute peak acceleration was identified, as illustrated for one passage at the second of the two IRJs in the time histories shown in Figures 2 and 3. These examples display the signal on the y-axis for a ±1 s interval around the estimated IRJ location, highlighting the distinct impact transient. The vertical dashed line in the time-history plots marks the estimated IRJ position based on coordinates before capturing the peak acceleration. To characterize impact energy, a RMS-value of the absolute amplitudes was computed in a ±1 ms window

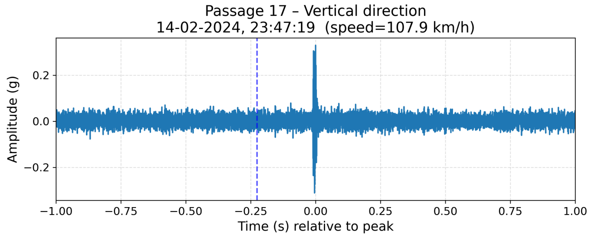

Figure 2: Ex. vertical acceleration signal at IRJ.

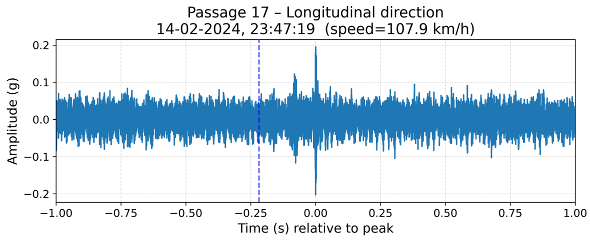

Figure 3: Ex. longitudinal acceleration signal at IRJ.

around the peak, as this isolates the high-frequency impulse typical of IRJ crossings which is too brief to be reliably represented by maximum absolute values alone. Both vertical (Z) and longitudinal (X) directions were analyzed, with X evaluated in a subwindow around the Z-peak to ensure co-located events. For each IRJ and direction, RMS values were plotted against speed and fitted with a second-order polynomial $f(v)$ where v is train speed. This model describes the expected speed-vibration response trend. Finally, regression models from the figures from these two IRJs were combined using a weighted approach based on passage counts to produce overall sensitivity estimates for Z and X directions. These combined models describe how speed influences amplitude when passing IRJs and allow calculation of sensitivity trends across the observed speed range.

To assess variability and potential condition effects, normalized RMS-values were calculated with Eq. (1).

$$RMS_{\text{norm}} = \frac{RMS_{\text{measured}}}{f(v)} \qquad (1)$$

Values above 1 indicate stronger than expected dynamic behavior, while values below 1 suggest weaker responses than expected from the passage speed. To contextualize potential deviations for these plots, a nationwide maintenance log from Bane NOR was examined, and relevant maintenance activities within the corresponding time period and track sections were extracted and included in the analysis.

This post-processing approach enables comparison between speed and acceleration amplitude across passages and supports the identification of outliers, addressing the third research question regarding the influence of conditions.

3. Axle-box Acceleration Analysis

3.1. RMS amplitude versus speed

Figures 4-7 illustrate the RMS responses as a function of speed for the two IRJs in vertical (Z) and longitudinal (X) directions. Both directions show increasing trends with speed. Vertical signals generally exhibit higher amplitudes than longitudinal signals. For both directions, the regression models indicate a near-linear increase across the observed speed range, although some curvature is present. Outliers are visible in both directions, with longitudinal responses showing greater variance from the fitted trend. This is reflected in the coefficient of determination R^2, which explains how well the regression model fits the relationship between speed and amplitude. Position 1 has $R^2 = 0.397$ for Z-direction and $R^2 = 0.275$ for X-direction while Position 2 has $R^2 = 0.501$ for Z-direction and $R^2 = 0.329$ for X-direction.

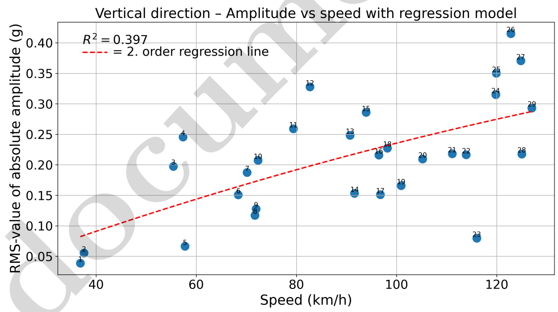

Figure 4: RMS acceleration versus speed - vertical direction for Position 1.

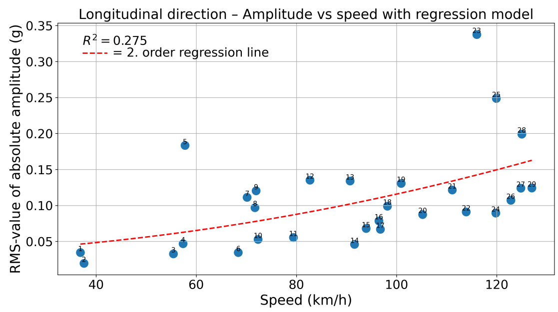

Figure 5: RMS acceleration versus speed - longitudinal direction for Position 1.

To provide an overall description of the speed–response relationship, regression models from the two IRJs were combined using a weighted approach based on passage counts. The resulting second-order polynomials for vertical (Z) and longitudinal (X) directions are shown in Eq. (2) and Eq. (3).

$$\bar{y}_Z(v) = 0.00000654\, v^2 + 0.00135\, v + 0.00567 \qquad (2)$$

$$\bar{y}_X(v) = 0.00000796\, v^2 + 0.0000713\, v + 0.04027 \qquad (3)$$

Both directions show a predominantly linear increasing

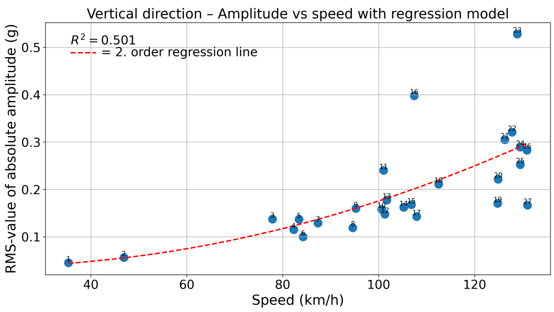

Figure 6: RMS acceleration versus speed - vertical direction for Position 2.

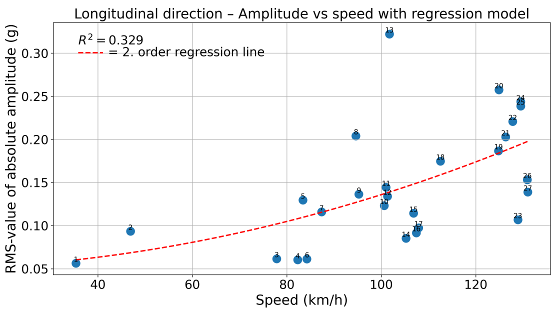

Figure 7: RMS acceleration versus speed - longitudinal direction for Position 2.

trend in amplitude with higher speed, although a slight curvature is present.
The sensitivity of RMS amplitude to speed was derived by differentiating the functions, shown in Eq. (4) and Eq. (5).

$$\frac{d\bar{y}_Z}{dv} = 0.0000131\, v + 0.00135 \tag{4}$$

$$\frac{d\bar{y}_X}{dv} = 0.0000159\, v + 0.0000713 \tag{5}$$

These derivatives quantify how RMS amplitude changes per unit increase in speed. Table 1 summarizes the estimated sensitivities for selected speeds. Both directions are more sensitive at higher speeds. Vertical acceleration shows roughly twice the sensitivity of longitudinal acceleration at moderate speeds (60–100 km/h), confirming its stronger correlation with speed. The difference between directions decreases with increasing speed, but Z remains more sensitive across the investigated speed range.

3.2. Normalized RMS evaluation

Figures 8-11 show the normalized RMS values for both IRJs and directions, sorted chronologically. Vertical dashed lines mark documented maintenance periods (rail grinding). The normalization removes the dominant speed influence and highlights passages with unusually high or low responses relative to the expected trends from the regression models in Figures 4-7.

v [km/h]	Z [g/(km/h)]	X [g/(km/h)]
35	0.00181	0.00063
60	0.00210	0.00100
80	0.00240	0.00135
100	0.00270	0.00170
130	0.00305	0.00214

Table 1: Estimated RMS sensitivity in vertical (Z) and longitudinal (X) directions.

The plots reveal substantial scatter, particularly in the longitudinal direction, and highlight several outliers exceeding the expected range. The vertical direction exhibits more consistent behavior, though isolated points deviate from the expected range. This is consisted with higher R^2-values for the vertical direction in both positions in Figures 4-7. Some reduction in normalized RMS-values after maintenance periods can be observed, especially in X-direction, and the regression models for the normalized Figures 9 and 11 support this trend, though R^2-values for these models are not very high due to many outliers and big variation from the correlation between speed and amplitude.
Overall, the normalized RMS evaluation supports identification of passages with atypical behavior and potential condition changes over time, addressing the third research question on track variability.

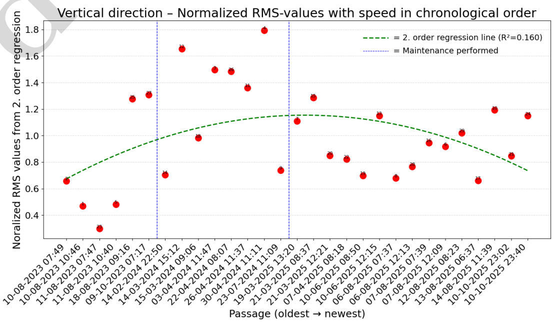

Figure 8: RMS vertical acceleration normalized with speed, including second-order regression in Position 1.

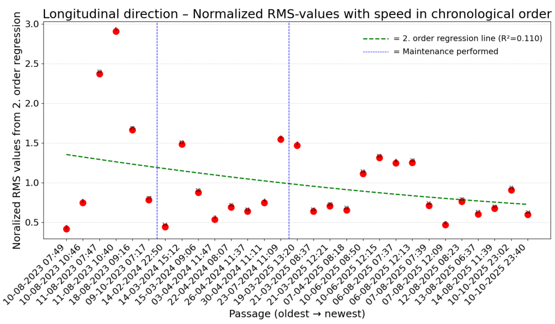

Figure 9: RMS longitudinal acceleration normalized with speed, including second-order regression in Position 1.

3.3. Visual inspection of the IRJs

In addition to these plots available images of the joints from 17 June 2025 were visually inspected. While the

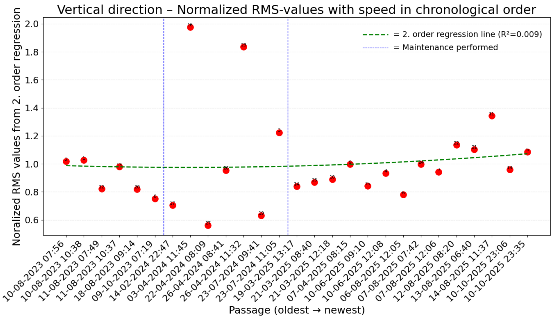

Figure 10: RMS vertical acceleration normalized with speed, including second-order regression in Position 2.

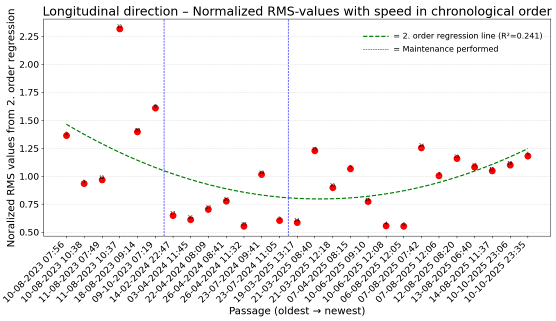

Figure 11: RMS longitudinal acceleration normalized with speed, including second-order regression in Position 2

images provide only limited diagnostic value, both joints appear generally intact, with no obvious surface defects visible at the resolution provided. Unfortunately, no other images of the IRJs were found.

4. Discussion

4.1. Discussion of the Results

The analysis confirms a clear and predominantly positive linear relationship between train speed and ABA amplitude at insulated rail joints, although some curvature is present in the regression models. Both IRJs show increasing RMS levels with speed, with vertical acceleration (Z) exhibiting higher amplitudes and a stronger correlation with speed than the longitudinal direction (X). This is consistent with the IRJ acting as a vertical stiffness discontinuity. The weighted regression models further quantify this behavior, showing that the sensitivity of the acceleration amplitudes in both directions increases with speed. The vertical direction (Z) is roughly twice as sensitive as the longitudinal direction (X) at moderate speeds (60-100 km/h), although the difference in sensitivity between the two directions decreases as speed increases.

Despite the overall trend, the relationship between speed and amplitude is not perfectly linear and exhibits significant scatter, reflected in the relatively low and varying R^2 values of the fitted regression models in Figs. 4–7. The scatter further indicates that ABA measurements are influenced by additional factors such as local track variation, wheel-rail interaction, or environmental conditions that differ between the two positions and time. As almost all passages at the two IRJs were from the same dates, the observed differences between positions are likely due to local track and geometry variations (+3.5‰vs -10‰gradient), and not operational differences. These observations align with previous studies showing that ABA responses, while clearly speed-dependent, are also sensitive to local conditions and can therefore contribute to detecting track irregularities.

Normalized RMS plots in Figs. 8-11 provide further insight by suppressing the dominant speed effect. They reveal periods with unusually high or low responses relative to the regression-based expectation, especially in the longitudinal direction. Some reduction in normalized values after documented rail grinding suggests a possible maintenance effect, especially in X-direction, where the normalized regression lines show a trend of decreasing amplitudes following grinding. In position 2 the model shows amplitudes rising again later when maintenance has not been performed for some time. However, the statistical fit remains weak due to high variability in responses when compensating for speed ($R^2 = 0.110$ and 0.241 for X-direction). This supports X-responses possibly being more sensitive to subtle variations in local track condition. Vertical responses show somewhat more stable behavior over time between speed and amplitude, in line with higher R^2 values in the amplitude-speed regressions (Figs. 4-7).

Although IRJs are nominally symmetric components, asymmetric wear or nearby track features may introduce train running direction-dependent responses, which were not investigated in this study. The influence of train running direction can therefore be a relevant topic for future work.

The observed differences between vertical and longitudinal responses, particularly the larger variability in the X-direction, suggest that directional sensitivity may contain additional diagnostic information. A more detailed study of direction-dependent mechanisms could therefore be valuable in future work.

4.2. Challenges

Several challenges influence the robustness of the results. GNSS uncertainty requires relatively wide windows in time or distance to locate the true impact event. Some sensors occasionally exhibit noise or anomalies. The study is limited to speeds up to only $\sim$ 130 km/h. The influence of the train running direction is unknown, and the modest number of passages increases the influence of outliers. Together, these factors reduce the statistical strength of the regression models and emphasize the need for larger datasets with a broader range of speeds and supplementary condition parameters (e.g., geometry measurements and train running direction) to better separate speed-related effects from true infrastructure changes. A significant restriction is the absence of systematic information about the IRJs' condition over time, making it difficult to determine whether variations in ABA response reflect true changes in joint condition or other operational factors, suggesting that more consistent condition documentation would be beneficial in future studies. It may also be advantageous to examine track defects with more defined condition states, such as squats, where the underlying damage mechanism is better understood, making it easier to quantify the effect of track condition on the correlation between speed and amplitude.

5. Conclusions and further research

This study analyzed the relationship between train speed and ABA response at two IRJs. The results confirm that speed is one of the primary factors affecting the vibration response. The main findings were:

- Acceleration increases nearly linearly with speed (35–130 km/h) in Z and X directions, with the largest signals observed in Z-direction for IRJs.
- Vertical acceleration shows the strongest correlation with speed and is $\approx 2\times$ as sensitive as longitudinal acceleration at moderate speeds (60-100 km/h). Although this difference decreases at higher speeds, Z remains the most sensitive direction across the speed interval 35-130 km/h.
- Since nearly all passages at both IRJs were from the same dates, differences in the amplitude-speed relationship in the two IRJs, which are reflected in the R^2-values (0.501 for Z and 0.329 for X vs 0.397 for Z and 0.275 for X), are likely due to local track and geometry variations rather than operational factors.
- Longitudinal accelerations displaying higher variability in the speed-amplitude relationship suggest that the X-direction is more sensitive to subtle changes in track condition than vertical direction. Normalized RMS trends and maintenance records further support that the X-direction is more sensitive to local condition changes.

ABA monitoring represents a promising tool for assessing IRJ condition. Future work should include more track geometry data (e.g. from Roger 1000), expanded datasets, a broader range of speeds, and examine more possible influencing factors as e.g. train direction, with increased focus on direction-dependent mechanisms between the X- and Z-directions in the analysis, to strengthen statistical confidence and better distinguish speed effects from true condition changes.

6. Acknowledgments

The authors acknowledge Bane NOR for data access.

References

[1] Z. Hu, A. Lau, J. Dai, and G. T. Frøseth, "Identification of optimal accelerometer placement on trains for railway switch wear monitoring via multibody simulation," eng, *Frontiers in Built Environment*, vol. 10, 2024, ISSN: 2297-3362. DOI: 10.3389/fbuil.2024.1396578.

[2] J. Flesjå, *Smart vedlikehold i Bane NOR*, eng, 2019. Accessed: Apr. 16, 2025. [Online]. Available: http://hdl.handle.net/11250/2620411.

[3] J. M. Castillo-Mingorance, M. Sol-Sánchez, F. Moreno-Navarro, and M. C. Rubio-Gámez, "A critical review of sensors for the continuous monitoring of smart and sustainable railway infrastructures," eng, *Sustainability 2020*, vol. 12, no. 22, pp. 9428–, 2020, ISSN: 2071-1050. DOI: 10.3390/su12229428.

[4] P. Salvador, V. Naranjo, R. Insa, and P. Teixeira, "Axlebox accelerations: Their acquisition and time–frequency characterisation for railway track monitoring purposes," *Measurement: journal of the International Measurement Confederation*, vol. 82, pp. 301–312, 2016, ISSN: 0263-2241. DOI: 10.1016/j.measurement.2016.01.012.

[5] H. Cho and J. Park, "Study of Rail Squat Characteristics through Analysis of Train Axle Box Acceleration Frequency," *Applied sciences 2021*, vol. 11, no. 15, pp. 7022–, 2021, ISSN: 2076-3417. DOI: 10.3390/app11157022.

[6] H. Cho, J. Park, and K. Park, "Analysis of axial acceleration for detection of rail squats in high-speed railways," *CivilEng*, vol. 4, pp. 1143–1156, 2023.

[7] Y. Zuo, J. Lundberg, P. Chandran, and M. Rantatalo, "Squat Detection and Estimation for Railway Switches and Crossings Utilising Unsupervised Machine Learning," eng, *Applied sciences 2023*, vol. 13, no. 9, pp. 5376–, 2023, ISSN: 2076-3417. DOI: 10.3390/app13095376.

[8] C. Yang, Y. Sun, C. Ladubec, and Y. Liu, "Developing Machine Learning-Based Models for Railway Inspection," eng, *Applied sciences 2021*, vol. 11, no. 1, pp. 13–, 2021, ISSN: 2076-3417. DOI: 10.3390/app11010013.

[9] M. Molodova, M. Oregui, A. Núñez, Z. Li, and R. Dollevoet, "Health condition monitoring of insulated joints based on axle box acceleration measurements," *Engineering Structures*, vol. 123, pp. 225–235, 2016.

[10] A. Malekjafarian, E. OBrien, P. Quirke, and C. Bowe, "Railway track monitoring using train measurements: An experimental case study," *Applied Sciences*, vol. 9, no. 22, p. 4859, 2019.

[11] L. Chia, B. Bhardwaj, P. Lu, and R. Bridgelall, "Railroad track condition monitoring using inertial sensors and digital signal processing: A review," *IEEE Sensors Journal*, vol. 19, no. 1, pp. 25–33, 2019.

[12] *Skjøter – Lærebøker i jernbaneteknikk*. Accessed: Apr. 16, 2025. [Online]. Available: https://www.jernbanekompetanse.no/wiki/Skj%C3%B8ter.